

IRON-OXIDE MAGMAS IN THE SYSTEM Fe-C-O

JERRY R. WEIDNER

*Department of Geology, University of Maryland, College Park,
Maryland 20742, U.S.A.*

ABSTRACT

The experimental determination of the iron oxide melting relations in a portion of the system Fe-C-O demonstrates that iron-oxide liquids can exist at geologically possible conditions. The existence of such liquids indicates that the "iron-oxide ore magma" hypothesis is a possible explanation for the origin of some iron ore deposits. Two invariant points and associated univariant equilibria involving iron-oxide liquids and graphite are experimentally located at pressures less than 2 kbar. The data also indicate the existence of two singular points. The invariant point most significant to the petrogenesis of an iron-ore magma is located at $815 \pm 10^\circ\text{C}$ and 0.3 ± 0.05 kbar, relating the phases magnetite, wüstite, graphite, liquid and vapor. The two univariant equilibria, originating at this invariant point and stable at higher pressure, are (a) wüstite + magnetite + graphite = liquid which changes to wüstite + graphite = magnetite + liquid at $880 \pm 6^\circ\text{C}$ and about 0.5 kbar and is linear, with a slope of $24^\circ\text{C}/\text{kbar}$, and (b) magnetite + graphite = liquid + vapor which passes through the T-P points $881 \pm 6^\circ\text{C}$ at 0.5 kbar, $918 \pm 6^\circ\text{C}$ at 1 kbar and $956 \pm 6^\circ\text{C}$ at 2 kbar. The latter reaction defines the minimum temperature necessary for liquid compositions most similar to natural iron-ore magmas. At 2 kbar, the composition of this univariant liquid lies in the three-phase triangle magnetite-wüstite-graphite and contains less than three mole % CO_2 . The calculated $f(\text{O}_2)$ is $10^{-13.2}$ atmospheres. These conditions are reasonable for some titaniferous iron-ore deposits associated with mafic rocks.

Keywords: iron-ore magma, iron-oxide liquids, system Fe-C-O, phase equilibria, magmatic iron ore.

SOMMAIRE

La détermination expérimentale des relations de fusion dans une portion du système Fe-C-O montre que les liquides enrichis en oxyde de fer sont stables dans des conditions géologiques plausibles. La preuve de l'existence de tels liquides étant faite, l'hypothèse d'un magma à oxyde de fer pourrait bien expliquer l'origine de certains gisements de fer. Deux points invariants et les équilibres univariants associés impliquant liquides d'oxyde de fer et graphite sont déterminés à une pression inférieure à 2 kbar. De plus, les données indiquent

l'existence de deux points singuliers. Le point invariant le plus pertinent à la pétrogénèse d'un magma à oxyde de fer se trouve à $815 \pm 10^\circ\text{C}$ et 0.3 ± 0.05 kbar; il implique les phases magnétite, wüstite, graphite, liquide et gaz. Deux équilibres univariants ont leur origine en ce point invariant et sont stables à pressions plus élevées: a) la réaction wüstite + magnétite + graphite = liquide, qui se transforme en wüstite + graphite = magnétite + liquide à $880 \pm 6^\circ\text{C}$ et environ 0.5 kbar; c'est une droite à coefficient angulaire de $24^\circ\text{C}/\text{kbar}$; b) la réaction magnétite + graphite = liquide + gaz, qui passe par les points $881 \pm 6^\circ\text{C}$ à 0.5 kbar, $918 \pm 6^\circ\text{C}$ à 1 kbar et $956 \pm 6^\circ\text{C}$ à 2 kbar. La deuxième réaction définit la température minimum nécessaire pour obtenir une composition de liquide la plus proche possible de celle de magmas à oxyde de fer naturels. À 2 kbar, la composition de ce liquide univariant se trouve dans le triangle marquant l'assemblage triphasé magnétite-wüstite-graphite et contient moins de 3% (molaire) de CO_2 . Pour la fugacité d'oxygène, le calcul donne $10^{-13.2}$ atmosphères. Ces conditions de formation sont raisonnables pour expliquer l'origine de gisements de Fe-Ti associés aux roches mafiques.

(Traduit par la Rédaction)

Mots-clés: minéral de fer magmatique, liquides à oxyde de fer, système Fe-C-O, équilibre de phase.

INTRODUCTION

The mechanism of formation and the very existence of iron-ore magmas have been controversial petrogenetic topics for many years. This report addresses the second part of the problem and describes the iron-oxide melting relations in part of the system Fe-C-O at pressures up to 2 kbar. The data presented here are part of a research program designed to evaluate the effect of volatile constituents on the melting relations of the iron-oxide minerals and the derivation of iron-oxide liquids from silicate magmas. The results of this study demonstrate that iron-oxide liquids can exist at geologically reasonable conditions.

Several considerations suggest the choice of the system Fe-C-O as the initial point of study. Many discordant dyke-like iron-ore bodies have

been interpreted as injections of residual iron-oxide magmas on the basis of field and petrographic criteria (*e.g.*, Geijer 1931, Lister 1966, Park 1972, Lundberg & Smellie 1979). This interpretation requires an iron-oxide liquid capable of existing independently of its parent silicate magma; the liquid should have the additional property of leaving the host rock virtually unaffected by contact-metamorphic processes. The ore magma must crystallize to an aggregate consisting largely of the iron-oxide minerals, which may or may not be titaniferous, lesser amounts of apatite (2–35%), plus very small quantities of silicate, carbonate and sulfide minerals. The refractory nature of such a combination of phases caused Geijer (1931) and many others to suggest that water, carbon dioxide or other mineralizers might lower the melting point of the iron-oxide minerals to geologically reasonable values in a manner analogous to the well-known behavior of silicate-water systems. If the El Laco (Chile) iron deposits are accepted as originating from "iron-oxide lava flows" (Park 1961, Haggerty 1970, Henriquez & Martin 1978), the highly vesicular nature of these "flows" indicates that they were charged with volatiles. However, it is unlikely that water alone would have the necessary effect. The rock-melting studies of Yoder & Tilley (1962), Piwinski (1974), Helz (1976) and many others have shown no evidence to suggest the existence of residual iron-oxide liquids.

Gibbon & Tuttle (1967) have shown that iron-oxide-rich melts occur in the Fe–SiO₂–O–H system at 1060°C, 2 kbar. It appears unlikely that these liquids could represent residual ore-magmas, since the temperature is well above the solidus of silicate rock–water systems at similar pressures. Philpotts (1967) reported that iron-oxide-rich apatite magmas could be derived from silicate magmas as immiscible liquids, but their temperature of melting (approximately 1400°C) appears to be unreasonably high for analogous natural magmas. On the other hand, carbonate minerals are ubiquitous, although minor, constituents of ore deposits of this type, and graphite has been reported (Anderson 1968). These observations suggest that carbon might play an important role in the evolution of iron-oxide magmas. The system Fe–C–O is the simplest possible system in which the iron-oxide melting relationships can be established as a function of pressure in the presence of a geologically reasonable volatile component. The phase equilibria in this simple system provide a foundation upon which the effect of additional com-

ponents, which more closely model nature, can properly be evaluated.

EXPERIMENT DESIGN AND TECHNIQUE

The experimental goal of this study is to identify and locate, in terms of pressure and temperature, the univariant and invariant equilibria involving iron-oxide liquids and graphite. Divariant equilibria were not systematically investigated because of two experimental limitations. Iron dissolves in noble-metal containers at high temperature; therefore, the bulk composition is not precisely known and changes continually during an experiment. Also, it is often difficult to consistently and unequivocally identify small amounts of primary crystals of oxide in a matrix of similar material quenched from a melt. However, topologically correct divariant relationships can be derived from the univariant and invariant data presented here, together with the phase-equilibrium data of Darken & Gurry (1945, 1946), Muan (1958), French & Eugster (1965) and published thermochemical data.

In general, bulk compositions were chosen so that the subsolidus assemblage consisted of three phases, *i.e.*, the assemblage was invariant at constant temperature and pressure. This greatly simplified the problem of interpretation because primary graphite, iron or vapor could be predicted and identified with reasonable confidence, leaving only a decision among primary wüstite, magnetite or liquid to be made. Under these conditions, oxygen fugacity $f(O_2)$ is a dependent variable and need not be explicitly measured or controlled.

The bounding binary systems have been extensively studied; thorough reviews are provided by Lindsley (1976) for Fe–O, Hansen & Anderko (1958) for Fe–C and French & Eugster (1965) for C–O. The ternary univariant reactions that have been located at one atmosphere and that are relevant to this study are listed in Table 1. Experimental work

TABLE 1. TERNARY UNIVARIANT REACTIONS LOCATED AT ONE ATMOSPHERE

M+G=W+V,	660° C	(Muan 1958)
W+G=I+V,	720° C	(Muan 1958)
W+I+V=L,	1371° C	(Darken & Gurry 1945)
W+V=M+L,	1424° C	(Darken & Gurry 1945)

Abbreviations used are: M magnetite, W wüstite, G graphite, I iron, V gas, L liquid.

on the ternary system at pressures above 0.1 kbar deals with equilibria involving siderite FeCO_3 (French 1971, Weidner 1972) and indicates that siderite is not stable at the T-P conditions of this study.

The following abbreviations will be used: H hematite, M magnetite, W wüstite, G graphite, V gas and L liquid. Where it is useful to distinguish among compositions of univariant liquids, a subscript indicating the stable subsolidus assemblage will be used; thus, L_{MGV} indicates the liquid produced when the subsolidus assemblage magnetite-graphite-vapor melts.

Apparatus

Two types of pressure vessels were used. Vertically mounted cold-seal vessels (Tuttle

1949) equipped with Bourdon-tube pressure gauges were used for all quench experiments at temperatures less than 900°C and pressures less than 1 kbar. New unsheathed Chromel-Alumel thermocouples were used for each experiment with these units. Internally heated pressure-vessels (Yoder 1950) equipped with Inconel-sheathed thermocouples and manganin pressure-sensing cells were used for the remainder of the experiments. All temperature-measuring systems were calibrated at the melting point of NaCl (800.5°C) at one atmosphere; the internally heated vessels were also checked against the melting point of gold (1066°C) at 0.5 kbar. The precision of temperature measurement and control is $\pm 5^\circ\text{C}$ or better. The temperature values reported are believed accurate to $\pm 10^\circ\text{C}$ or better. All pressure-measuring

TABLE 2. RESULTS OF DEFINITIVE EXPERIMENTS

Run No.	Comp. (mole %)	T°C	P Kb	t(hrs.)	Results	Reagents Used
0528	Fe=54, O=27, C=19	975	2	29	L+G+V	Fe_2O_3 : Graphite
0529	" "	962	2	29	L+G+V	"
0530	" "	950	2	24	M+G+V	"
0531	" "	925	2	9.5	M+G+V	"
0611	" "	950	1	15	L+G+V	"
0612	" "	925	1	14	L+G+V	"
0714	" "	912	1	54	M+G+V	"
0668	" "	950	0.5	30	L+G+V	"
0670	" "	900	0.5	29	L+G+V	"
0672	" "	887	0.5	32	L+G+V	"
0673	" "	875	0.5	32	M+G+V	"
0824	" "	950	0.25	28	L+G+V	"
0825	" "	925	0.25	36	L+G+V	"
0826	" "	900	0.25	27	L+G+V	"
0827	" "	875	0.25	25	L+G+V	"
0828	" "	850	0.25	48	L+G+V	"
0829	" "	825	0.25	40	L+G+V	"
0831	" "	805	0.25	44	M+G+V	"
0555	Fe=80, O=15, C=5	1000	2	8	L+V	Fe_2O_3 : FeCO_3 : Fe
0556	" "	975	2	29	L+V	"
0557	" "	950	2	24	L+M+G	"
0558	" "	925	2	9.5	L+M+G	"
0559	" "	912	2	38	M+W+G	"
0560	" "	900	2	28	M+W+G	"
0618	" "	950	1	15	L+V	"
0619	" "	925	1	14	L+V	"
0620	" "	900	1	24	M+G+L	"
0621	" "	887	1	32	M+W+G	"
0622	" "	875	1	43	M+W+G	"
0675	" "	925	0.5	28	L+V	"
0676	" "	900	0.5	29	L+V	"
0677	" "	887	0.5	32	L+V	"
0678	" "	875	0.5	32	M+W+G	"
0762	" "	860	0.5	50	M+W+G	"
0834	" "	900	0.25	27	L+V	"
0835	" "	875	0.25	25	L+V	"
0836	" "	850	0.25	48	M+L+V	"
0837	" "	825	0.25	48	M+W+V	"
0831	" "	805	0.25	44	M+G+V	"
0639	Fe=51, O=37, C=12	900	1	24	L+I+G	FeCO_3 : Fe
0641	Fe=51, O=48, C=1	887	1	32	L+I+G	Fe_2O_3 : FeCO_3 : Fe
0640	Fe=51, O=37, C=12	850	1	24	I+W+G	Fe_2O_3 : Fe
0787	" "	900	0.5	27	L+M+G	"
0785	" "	850	0.5	41	I+W+G	"
0856	" "	875	0.25	42	L+I+G	"
0858	" "	825	0.25	40	I+G+V	"
0502	Fe=3.4, O=5.2, C=91.4	1025	0.34	1	L+G+V	Fe_2O_3 : Graphite
0500	" "	1025	0.23	1	I+G+V	"

Abbreviations used are: M=magnetite, W=wüstite, G=graphite, V=gas, I=iron, L=liquid. The results column indicates the assemblage stable at the conditions of the experiment.

devices were calibrated against a Heise Bourdon-tube gauge accurate to 0.1%. Reported values of pressure are accurate to $\pm 5\%$ or better.

Initial quench-rates were about $300^{\circ}\text{C}/\text{minute}$ for cold-seal vessels and about $200^{\circ}\text{C}/\text{minute}$ for internally heated vessels. Pressure decreased to about 70% of the experiment value during the quench. Argon was the pressure medium used in all definitive experiments listed in Table 2.

Starting materials

Siderite was prepared by heating $\text{FeC}_2\text{O}_4 \bullet 2\text{H}_2\text{O}$ (Matheson, Coleman and Bell, C.P. grade) at 380°C and 3 kbar for forty-eight hours using unsealed gold capsules in a 97% CO_2 -3% CO atmosphere. The grain size of siderite ranged from 0.5 to $10 \mu\text{m}$. Hematite Fe_2O_3 (Fisher Certified Reagent, lot 792499) was heated in air at 700°C for 48 hours and had a final grain-size of $< 1 \mu\text{m}$. Graphite (Union Carbide Co., spectrographic grade, 80% < 200 mesh) was dried in air at 110°C to constant weight. Iron (Leytess Metal and Chemical Co., assay 99.9%, grain size 20–50 μm) was used as received.

Starting mixes were one-gram mechanical mix-

tures prepared by homogenizing manually, in air, weighed amounts of the appropriate reagents in an agate mortar for about fifteen minutes. The level of oxygen contamination, both from surface oxide on the iron and air trapped in sealed capsules, was checked by heating mixtures of iron and hematite (bulk composition: Fe_2O_4) in sealed silver capsules at 700°C , 1 kbar, for forty-eight hours. Magnetite is virtually stoichiometric under these conditions (Greig *et al.* 1935). Examination of polished sections after heating indicated the hematite content to be $< 0.1\%$, which was judged insignificant.

Different combinations of reagents have no effect on the experimental results. This observation indicates that equilibrium was attained and that the synthesis experiments used in this study are appropriate. The apparatus allowed either four or eight samples to be heated simultaneously. In every heating experiment, at least two mixes had identical compositions, but were prepared from different reagents. In the composition triangle Fe_3O_4 – graphite – CO_2 , Fe_2O_3 – graphite mixes were compared with FeCO_3 –Fe mixes. FeCO_3 –Fe mixes were compared with Fe_2O_3 – Fe – graphite mixes in the composition triangles $\text{FeO} - \text{Fe}_3\text{O}_4 - \text{graphite}$ and $\text{FeO} - \text{Fe} - \text{graphite}$ (Fig. 1). The bulk compositions are shown in Figure 1, together with the subsolidus

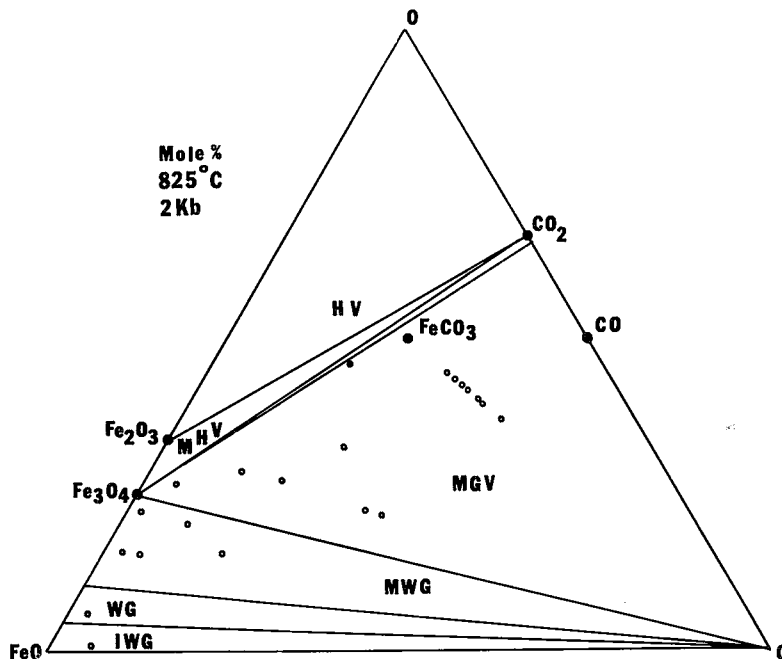


FIG. 1. Isothermal-isobaric section showing the composition of starting mixtures and the stable three-phase and two-phase assemblages.

phase-assemblages stable at 825°C and 2 kbar. Some bulk compositions near the Fe-C sideline are not shown.

Sample containers

Sealed sample containers of Ag_6Pd_4 alloy were used for most experiments as an acceptable compromise between high-temperature stability and minimum iron-loss (Muan 1963). Experiments at temperatures above 1100°C required platinum capsules; iron loss was minimized by using a spectroscopic-grade graphite crucible within the sealed container. The possibility that the container material was soluble in the oxide liquid was checked by comparing melting-point data from duplicate experiments using Ag, Au, Pt and Ag_6Pd_4 capsules and, also, by examining polished sections for evidence of capsule-metal precipitation from the oxide melts. The different capsule-materials gave identical results, and no evidence of capsule-metal solubility in the oxide liquids was observed.

Containers were fabricated from tubing 2.5 mm in outer diameter, filled with 20 to 40 mg of starting material, and sealed by carbon-arc welding. The filled capsules were flattened prior to the final welding in order to minimize the amount of trapped air.

Analytical procedures

Quenched samples were characterized using a binocular stereoscopic microscope, a petrographic microscope (reflected and transmitted light) and a Norelco X-ray powder diffractometer equipped with a copper tube and LiF monochromator. The degree of capsule puffing was noted before the containers were opened. The presence of gas under pressure was indicated by the evolution of bubbles when the containers were pierced under acetone. Major textural features, such as vesiculation, the presence and location of microphenocrysts, meniscus and spherulites, were established using the binocular microscope after the sample had been removed intact from the container. The sample was then broken into two pieces; one was studied in polished section, the other was examined using X-ray powder-diffraction techniques and transmitted-light microscopy.

ANALYSIS AND INTERPRETATION OF PRIMARY PHASES

The phases and textures found in quenched samples are described in the following section.

L_{MGV}

Melting among the phases magnetite-vapor-graphite is indicated by a very distinct textural change. If hematite-graphite or siderite-graphite starting mixtures are used, the subsolidus charges are physically incoherent aggregates of graphite and very fine-grained magnetite ($< 1 \mu\text{m}$). For starting materials containing metallic iron, the textures in subsolidus experiments are identical to those described above, except for irregular to oval domains 10–100 μm across of magnetite "pseudomorphs" after metallic iron. In contrast, melted charges contain 20–100 μm ameboid masses of magnetite and many spherical to ameboid voids up to 100 μm across. The texture closely resembles that of a common household sponge in miniature. In many cases, a deep concave depression is preserved at one end or side of the charge, indicating a liquid-gas meniscus. The texture of samples quenched from temperatures 25 to 100°C above the melting temperature is identical to the above, except that wüstite is the dominant quench-product. In this case, magnetite occurs as irregular patches within the wüstite and as rims on the edges of the wüstite aggregate. The textural change is sufficient to locate the temperature of the melting reaction with a precision of $\pm 6^\circ\text{C}$ at all pressures investigated. In all cases the quenched sample-containers are puffed and contain a gas at a pressure greater than one atmosphere.

L_{WMG}

The quench textures of samples in the composition triangle magnetite-wüstite-graphite are, in general, very similar to the textures described above. The characteristic subsolidus texture involves 10–100 μm irregular to oval pseudomorphs of wüstite or magnetite (or both) replacing the metallic iron in the starting materials, set in a very fine-grained ($< 1 \mu\text{m}$) ground-mass of wüstite and magnetite. The quench liquids are also vesiculated, but to a lesser degree, and generally possess a meniscus. The L_{WMG} experiments differ from the L_{MGV} in that: (1) the L_{WMG} quenched liquids always consist of wüstite with irregular patches of magnetite, distributed both within the wüstite aggregates and on the vesicle edges; (2) the capsules from subsolidus L_{WMG} experiments are always flat and tightly molded around the sample, whereas the capsules from hypersolidus runs are usually slightly puffed around the charge. The melting reaction is experimentally located with a precision of $\pm 6^\circ\text{C}$ at all pressures investigated.

L_{MWG}

The characteristics of oxide liquids formed from the assemblage metallic iron, wüstite, graphite are much more poorly defined than those noted above. Melted samples are not vesiculated, and the containers are tightly molded around both subsolidus and hypersolidus samples. Three criteria were used to establish melting. A given experiment was judged to be definitive only if all three criteria were satisfied. On this basis, the isobaric melting temperature could be located with a precision of $\pm 25^\circ\text{C}$. The criteria are: 1) Graphite produced by the decomposition of siderite in the starting material is very fine-grained ($< 1 \mu\text{m}$) and homogeneously distributed in subsolidus samples, but tends to form lumps and aggregates in hypersolidus charges. 2) Subsolidus assemblages are physically incoherent, whereas hypersolidus assemblages are coherent. 3) In subsolidus experiments, the metallic iron occurs as 10 to 20 μm spherical grains homogeneously distributed through the sample. In hypersolidus experiments, it occurs only as a thin iron-rich alloy (with palladium) at the charge-capsule interface. Iron is lost from the samples by alloying with the Ag-Pd containers during both hypersolidus and subsolidus experiments. Criterion 3 is based on the observation that a sharp, discontinuous increase in the rate of iron loss occurs with increasing temperature. It is probably related to the increased ionic diffusivity and electrical conductivity of the melt compared to the crystalline aggregate. Criterion 3 is only applicable if the capsule is Ag₆Pd₄ alloy and the experiment lasts 24 to 48 hours. In contrast, experiments using containers of silver, which does not form an iron alloy, were identical in all respects, except that the metallic iron remained homogeneously distributed.

Vapor

The presence or absence of vapor during an experiment is usually indicated by the capsule configuration. The capsule walls are not welded together if vapor is present during the experiment. In contrast, vapor-absent assemblages typically produce containers that are flat and either tightly molded about the charge or slightly puffed around the sample only. The slight puffing of the container is characteristic of quenched L_{MWG}. In this case, metastable gas is evolved during the quench, rather than the stable subsolidus phase graphite, and produces vesiculated textures and often a well-developed meniscus. Thus the presence of vesicles or a

meniscus (or both) is good evidence for the former presence of a liquid, but not a vapor, during an experiment. The capsule walls are typically coated with a thin film of carbon, suggesting that the metastable vapor is CO-rich and disproportionates into CO₂ and carbon during the quench of L_{MWG}.

Magnetite

Primary magnetite occurs as small (1–10 μm), equant, euhedral grains in subsolidus and vapor-absent assemblages, but as larger (50–100 μm), equant, euhedral microphenocrysts when liquid and vapor are present. Often the magnetite microphenocrysts are concentrated at the bottom of the charge, indicating crystal settling in a low-viscosity liquid. Magnetite quenched from liquid occurs as irregular masses (20–100 μm) containing numerous spherical to amoeboid voids.

Wüstite

Wüstite exhibits a great variability in habit, but no generally applicable criteria were developed to distinguish primary wüstite from that produced from quenched liquid. However, L_{MWG} assemblages provided two exceptions to this generalization. Spherulitic aggregates of acicular wüstite crystals were often found at the liquid-capsule interface. Also, rarely, the X-ray diffractograms showed doublets of wüstite peaks, indicating the presence of two different wüstite compositions and suggesting the former presence of primary wüstite and liquid.

Iron

Primary iron occurs as 10 to 20 μm spherical to ovoid grains that contain laths of cementite (Fe₃C).

Graphite

Primary graphite occurs in two distinct size-populations. Large (30–150 μm), irregular shards are inherited from graphite in the starting material, whereas very small ($< 1 \mu\text{m}$) grains are produced by the decomposition of siderite used in the starting mixtures.

Metastable crystalline phases

Cementite is observed as laths in iron. It is regarded as a metastable phase because all run products in which cementite developed were not only saturated with graphite, but also contained

iron. If cementite were stable, iron should not be present. This interpretation is consistent with the data published on the system Fe-C (Hansen & Anderko 1958). Graphite-saturated γ -iron contains about 0.65 wt.% C at 738°C and 2 wt.% C at 1152°C. Graphite-saturated α -iron, stable at temperatures less than 738°C, is virtually carbon-free. During quenching, particularly at the cooling rates used in this study, metastable Fe_3C is exsolved from the iron solid-solution rather than the stable phase graphite [see Chipman (1974) for additional discussion].

Traces of an unidentified phase are observed in several subsolidus and hypersolidus runs where vapor is present. This material occurs as very small ($< 1 \mu\text{m}$), transparent, birefringent grains and as rims on magnetite; it has X-ray-diffraction peaks at 2.225 and 1.926 Å. The indices of refraction could not be accurately determined, but appear to be similar to those of siderite. It was not identified in polished section. This material is interpreted as a metastable product formed during quenching because it was not observed at temperatures less than about 750°C; it has not been reported in studies of siderite equilibrium (French 1971, Weidner 1972); it does not increase in amount as a function of time, and it is present in a given sample only if vapor also is present.

RESULTS AND DISCUSSION

The success of this study hinges on the correct interpretation of the textural features described above. Thermochemical calculations, neglecting the possibility of melting, indicate that the reaction magnetite + graphite = wüstite + vapor should occur at temperatures and pressures comparable to the appearance of the textural features that are interpreted as indicating quenched oxide liquids. The textural features, interpreted as due to melting, could instead be due to the sintering of wüstite in the presence of a gas phase under pressure. The presence of magnetite could be explained as due to oxidation during quenching. Two lines of evidence, independent of the textural features, indicate that the melting interpretation is correct.

Consider the three-phase assemblages magnetite-graphite-vapor and magnetite-wüstite-graphite (see Fig. 1) at 2 kbar. These assemblages are stable at temperatures less than the possible magnetite + graphite = wüstite + vapor reaction. At temperatures higher than the univariant equilibrium, the magnetite-graphite join is not stable, and both assemblages

change to wüstite-graphite-vapor, provided graphite is present in excess. However, the textural change interpreted as melting occurs at $956 \pm 6^\circ\text{C}$ in the magnetite-graphite-vapor assemblage and at $918 \pm 6^\circ\text{C}$ in the magnetite-wüstite-graphite assemblage. Since the texture change is reproducible to $\pm 6^\circ\text{C}$ for both assemblages, it is apparent that it cannot be due to the reaction $\text{magnetite} + \text{graphite} = \text{wüstite} + \text{vapor}$.

If melting does occur, then the quench experiments indicate that it, and the subsequent crystallization during cooling, must occur very rapidly and should be detectable using differential thermal analysis (DTA) techniques. Qualitative DTA experiments were made in the 1 to 5 kbar range using magnetite-graphite-

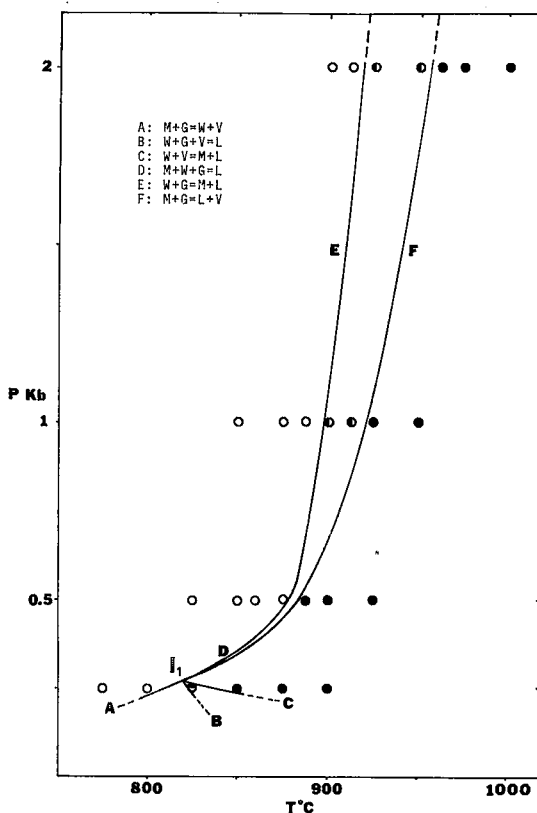


FIG. 2. T-P projection showing the results of experiments locating invariant point I_1 and associated univariant curves. Filled circles indicate the assemblages $M+L+V$, $L+V$, $G+L+V$. Left-half-filled circles indicate the assemblages $M+G+V$, $M+G+L$. Top-half-filled circles indicate the assemblages $W+M+V$, $G+L+V$. Open circles indicate the assemblages $M+W+G$, $M+G+V$.

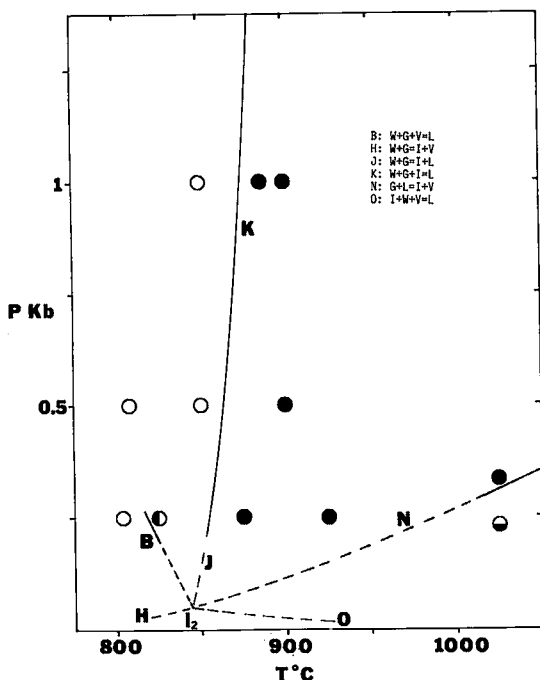


FIG. 3. T-P projection showing the results of experiments locating invariant point I_2 and associated univariant curves. Filled circles indicate the assemblage $I+G+L$. Left-half-filled circles indicate the assemblages $I+W+G$, and $G+L+V$. Bottom-half-filled circles indicate the assemblage $I+G+V$. Open circles indicate the assemblage $I+W+G$.

vapor, magnetite-wüstite-graphite and iron-wüstite-graphite subsolidus assemblages. Thermal effects consistent with melting and subsequent crystallization were observed on the heating and cooling cycles at temperatures comparable to the texture change observed in quench samples. The slopes of the pressure-temperature curves for the DTA data are the same as those obtained from the texture-change data obtained from quench experiments. The bulk compositions magnetite-graphite-vapor and magnetite-wüstite-graphite gave particularly strong, sharp, exothermic effects when cooled from 1100°C at 200°C/minute, exactly as expected if supercooled liquids abruptly crystallize and exsolve a gas phase. This is contrary to the expected behavior of the reaction $\text{magnetite} + \text{graphite} = \text{wüstite} + \text{vapor}$, because magnetite is a minor component when these compositions are quenched from 1000°C or higher temperatures; therefore, the exothermic heat effect produced by oxidation of wüstite

to magnetite during the quench would be much smaller in magnitude than the magnetite-reduction reaction during heating, and would also be spread over a broad range of temperature.

Invariant and univariant equilibria

The invariant and univariant equilibria are obtained from the experimental results and an analysis of the data using the method of Schreinemakers (1915-1925). The experimental results are shown in P-T projection in Figures 2 and 3. The results of experiments on selected compositions are listed in Table 2. Table 3, a complete list of experimental results, is available from the Depository of Unpublished Data, CISTI, National Research Council of Canada, Ottawa, Ontario K1A 0S2. The data indicate two invariant points in the temperature range 800 to 875°C at less than 0.5 kbar and suggest that two singular points are located at pressures slightly higher and lower, respectively, than this

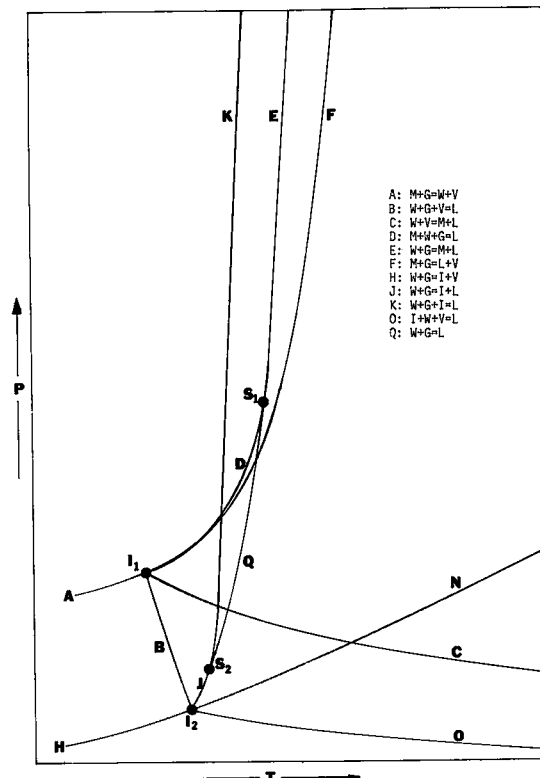
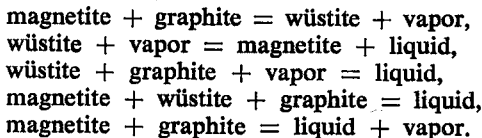


FIG. 4. T-P projection showing the relation between invariant points I_1 and I_2 , singular points S_1 and S_2 and associated univariant reactions.

value. Figure 4 is a schematic P-T projection showing the relationship between the two invariant points, the two singular points and the univariant curves.

Invariant point I_1

Invariant point I_1 among the phases magnetite-wüstite-graphite-liquid-vapor is located at $815 \pm 10^\circ\text{C}$ and 0.3 ± 0.05 kbar by a short extrapolation of the experimentally determined univariant curves (Fig. 2). It is the origin of the univariant reactions:



The first three reactions are experimentally located at 0.25 kbar and related to lower-pressure equilibria in the following ways: magnetite + graphite = wüstite + vapor originates at an invariant point among the phases iron, wüstite, magnetite, graphite and vapor at a pressure less than one bar and passes through the point 660°C at one bar (Muan 1958); wüstite + vapor = magnetite + liquid has a sharply negative slope and passes through the T-P point 1424°C , one atm (Darken & Gurry 1945, 1946); wüstite + graphite + vapor = liquid has a negative slope and terminates at invariant point I_2 , which is described below. The remaining two reactions, magnetite + wüstite + graphite = liquid and magnetite + graphite = liquid + vapor, are stable above 0.3 kbar. The data suggest that the eutectic reaction magnetite + wüstite + graphite = liquid changes to the peritectic reaction wüstite + graphite = magnetite + liquid at about 880°C , 0.5 kbar. It is linear, within experimental error, with a slope of $24^\circ\text{C}/\text{kbar}$ between 0.5 and 2 kbar. Liquid compositions lie in the $\text{FeO}-\text{Fe}_3\text{O}_4-\text{C}$ composition triangle at temperatures less than 1000°C and pressures equal to or less than 2 kbar. The CO_2 content of the liquid is less than 3 mole %.

Invariant point I_2

Invariant point I_2 is located at $850 \pm 30^\circ\text{C}$ and less than 0.25 kbar by extrapolation of the experimentally located curves wüstite + graphite + vapor = liquid, wüstite + graphite = iron + liquid and liquid + graphite = iron + vapor (Fig. 3). The two additional univariant reactions intersecting at this invariant point are wüstite + graphite = iron + vapor and wüstite + iron + vapor = liquid. They were not investigated in this study, but are known

from the one-atmosphere phase relations (Darken & Gurry 1945). Wüstite + graphite + vapor = liquid has a negative slope and is common to I_1 and I_2 . Liquid + graphite = iron + vapor terminates at $1142 \pm 5^\circ\text{C}$, 0.53 ± 0.05 kbar at an invariant point among the phases oxide liquid, metallic liquid, iron, graphite, vapor (J. Weidner, unpubl. data). The reaction wüstite + graphite = iron + liquid could be located with a precision of $\pm 25^\circ\text{C}$ at a given pressure. The data indicate that the slope is slightly positive below 0.5 kbar and essentially vertical at higher pressures and suggest that the peritectic reaction changes to the eutectic type: wüstite + graphite + iron = liquid.

Singular phenomena

In the above description, it was suggested that wüstite-graphite-iron-liquid and wüstite-magnetite-graphite-liquid univariant equilibria change order, *i.e.*, the reactions change from peritectic to eutectic type. This proposal stems from the observation that these univariant reactions intersect and change slope in P-T space at about 880°C and 0.5 kbar (note experiments 0621 and 0641 in Table 2). In general, ternary systems, such as Fe-C-O, require that the lowest melting temperature assemblage at any given pressure be of the eutectic type. At 1 kbar, wüstite-graphite-iron is the low-melting assemblage, and the melting reaction must be wüstite + graphite + iron = liquid. At 0.25 kbar, wüstite-graphite-vapor is the low-melting assemblage, and the position of this univariant curve in P-T space requires the reactions to be magnetite + wüstite + graphite = liquid at I_1 and wüstite + graphite = iron + liquid at I_2 . The change from wüstite + graphite = iron + liquid (at 0.25 kbar) to wüstite + graphite + iron = liquid (at 1 kbar) indicates that a singular point (S_2 in Fig. 4) exists between these pressures. At this point, the liquid composition becomes collinear with wüstite and graphite; it is the origin of the degenerate reaction wüstite + graphite = liquid. The degenerate reaction terminates at a singular point (S_1 in Fig. 4), where the reaction magnetite + wüstite + graphite = liquid changes to wüstite + graphite = magnetite + liquid. The location of the second singular point is suggested by the change in slope at about 880°C and 0.5 kbar shown by this vapor-absent reaction (Fig. 4). Note that the intersection of the other curves shown in Figure 4 occurs in P-T projection only.

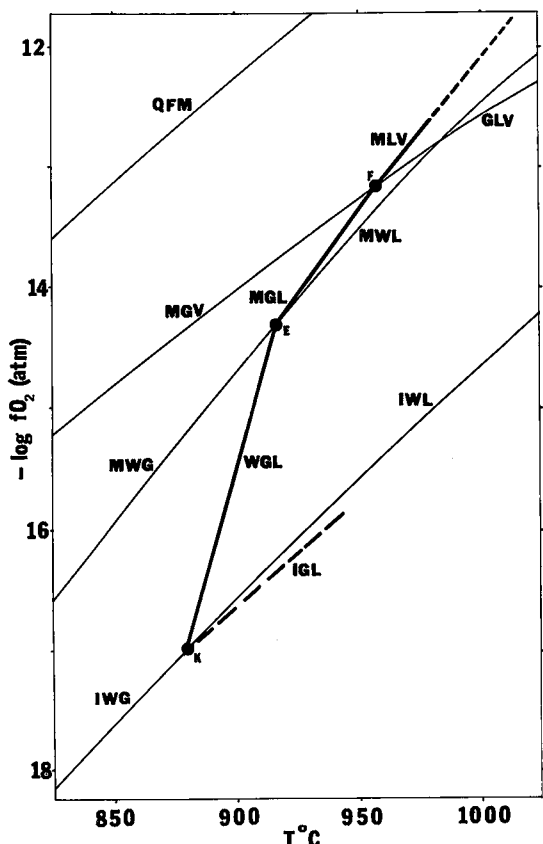


FIG. 5. $T-f(O_2)$ projection at 2 kbar showing the univariant and divariant equilibria. The heavy lines define the field boundary of liquid. QFM is the quartz-fayalite-magnetite $f(O_2)$ buffer (Chou 1978).

Divariant equilibria

Divariant equilibria are derived from the data presented here together with the available thermochemical data. An isobaric $T-f(O_2)$ projection at 2 kbar is shown in Figure 5. Three univariant equilibria involving oxide liquids are stable at temperatures less than 1000°C; each is the intersection of four divariant surfaces. In isobaric projection, these appear as points and lines, respectively. Two of the divariant equilibria intersecting each isobaric invariant point are familiar $f(O_2)$ buffer assemblages: graphite-vapor (French & Eugster 1965) defines the position of the magnetite-graphite-vapor and graphite-liquid-vapor curves about the univariant reaction magnetite + graphite = liquid + vapor; similarly, the wüstite-magnetite (WM) $f(O_2)$ buffer (Eugster & Wones 1962)

defines the location of the wüstite-magnetite-graphite and wüstite-magnetite-liquid surfaces about the reaction wüstite + graphite = magnetite + liquid; the wüstite-iron (WI) $f(O_2)$ buffer (Eugster & Wones 1962) defines the location of the iron-wüstite-graphite and iron-wüstite-liquid divariant equilibria about the reaction iron + wüstite + graphite = liquid. Magnetite-graphite-liquid and wüstite-graphite-liquid are each common to two isobaric invariant points and must pass between these points with some undetermined curvature. The curve magnetite-liquid-vapor is not located precisely, but must be located between the metastable extension of the magnetite-graphite-liquid curve and the stable graphite-liquid-vapor assemblage, and also must diverge from the magnetite-wüstite-liquid curve at higher temperatures and $f(O_2)$ values (Fig. 5). The position of the curve iron-graphite-liquid is schematic; it is required only to pass through point K and lie between the metastable extension of wüstite-graphite-liquid and the stable portion of iron-wüstite-liquid. Note that, although the absolute magnitude of the calculated $f(O_2)$ values is probably not known to better than ± 0.2 log units, the relative position of the curves is correct as shown, and the calculated topology is consistent with the results of this study. The quartz-fayalite-magnetite (QFM) $f(O_2)$ buffer (Chou 1978) is included for comparison.

At 2 kbar, the low-temperature boundary of the stability field of liquid is defined by the curves magnetite-liquid-vapor at temperatures greater than 956°C and magnetite-graphite-liquid at lower temperatures to 918°C. Both assemblages have $f(O_2)$ values somewhat above the wüstite-magnetite $f(O_2)$ buffer, but much less than the QFM buffer at temperatures less than 1000°C. At $f(O_2)$ values less than the WM buffer, the minimum temperature of the field boundary of liquid is defined by the curve wüstite-liquid-graphite between 918 and 880°C and by the iron-liquid-graphite curve at higher temperatures and $f(O_2)$ values slightly less than the IW buffer. The iron-liquid-graphite equilibrium terminates at the isobaric invariant point among the phases oxide liquid, metallic liquid, iron and graphite at $1142 \pm 5^\circ\text{C}$ (J. Weidner, unpubl. data).

Petrogenetic implications

The phase equilibria described in the preceding section demonstrate that iron-oxide liquids can exist at reasonable magmatic temperatures through a broad range of P and $f(O_2)$ values.

However, if it is assumed that an iron-ore deposit is genetically related to a host silicate rock, then the liquids shown in Figure 5 at $f(O_2)$ values less than those of the WM buffer can, for general purposes, be eliminated from consideration as models for natural ore-magma. Both wüstite and iron-oxide liquid, at comparable $f(O_2)$ values, are unstable with respect to ferrous silicate minerals unless the host rock is extremely silica-deficient. The following observations suggest that liquids located in the $f(O_2)$ region above the WM buffer (Fig. 5) may be regarded as simplified iron-ore magmas.

The liquids have $f(O_2)$ and temperature values within the range of mafic rocks (Haggerty 1976) and are virtually identical to many of the $f(O_2)$ estimates of Williams (1971) for the Skaergaard complex (Greenland). According to the compilation of $f(O_2)$ data of Haggerty (1976), titaniferous magnetite deposits have an approximate $f(O_2)$ range of one log unit above to two log units below the QFM buffer curve shown in Figure 5, with values distributed virtually parallel to it. If these data are extrapolated to higher temperatures parallel to the QFM buffer curve, the lower range of $f(O_2)$ values is very similar to that considered for the liquids here.

Graphite, although rare, has been reported in several igneous complexes, including the Skaergaard (Greenland), Stillwater (Montana), Bushveld (South Africa) (Elliot *et al.* 1981) and Duluth (Minnesota) (Mainwaring & Naldrett 1977, Hollister 1980) and in the La Blache Lake (Quebec) titaniferous magnetite deposit, (Anderson 1968). However, graphite would not necessarily be present in an ore deposit derived from natural melts comparable to those reported here. If the ore magma is similar to the liquid defined by the region between the magnetite-liquid-vapor and graphite-liquid-vapor curves (Fig. 5), and if the $f(O_2)$ of crystallization of the ore magma is buffered at a value above the graphite-vapor equilibrium by the host silicate rock, then magnetite and vapor are the only subsolidus products. This conclusion holds for pressures above 0.3 kbar. At lower pressures, magnetite and vapor are the only subsolidus products if the liquid is maintained at an $f(O_2)$ value above that set by the WM buffer during the crystallization process.

The location of the stability field of liquid below the QFM buffer (Fig. 5) indicates that natural ore-magma analogues would probably coexist only with rocks undersaturated in silica. This is consistent with the occurrence of nepheline syenite in the anorthositic complex asso-

ciated with the La Blache Lake magnetite deposits (Anderson 1968). This generalization is valid for temperatures less than 1000°C. The situation at higher temperatures is uncertain and depends on the slope of the magnetite-liquid-vapor surface in T- $f(O_2)$ space (Fig. 5). This does not eliminate the possibility that iron-ore magmas could exist with silica-oversaturated rocks at temperatures less than 1140°C, the one-atmosphere melting temperature of the QFM buffer-assemblage (Muan 1955).

The analogy between the liquids described in this report and natural iron-ore deposits is based on the assumption that additional components will not change the phase relations significantly. The assumption is reasonable if the additional components are small in amount and do not cause the formation of additional phases. The one-atmosphere melting data in the system $FeO-Fe_2O_3-TiO_2$ (Taylor 1963) indicate that the slope of the spinel liquidus-surface decreases with increasing titanium content. Philpotts (1967) showed that apatite lowers the melting temperature of the iron-oxide minerals in the pseudoternary system "diorite-magnetite-apatite" by about 200°C at one atmosphere. If these generalizations are applicable at higher pressures with carbon as an additional component, then titaniferous iron-ore magma could exist at temperatures somewhat lower than those reported here.

ACKNOWLEDGEMENTS

The experimental work described here was carried out in the experimental petrology laboratories at Stanford University, Goddard Space Flight Center and the University of Maryland. Financial support was provided by the National Science Foundation and the National Aeronautic and Space Administration. The comments of the referees were most helpful.

REFERENCES

- ANDERSON, A.T., JR. (1968): Oxidation of the La Blache Lake titaniferous magnetite deposit, Quebec. *J. Geol.* **76**, 528-547.
- CHIPMAN, J. (1974): C-Fe (carbon-iron). In *Metals Handbook* (8th ed., vol. 8). American Society for Metals, Metals Park, Ohio.
- CHOU, I-MING (1978): Calibration of oxygen buffers at elevated P and T using the hydrogen fugacity sensor. *Amer. Mineral.* **63**, 690-703.
- DARKEN, L.S. & GURRY, R.W. (1945): The system iron-oxygen. I. The wüstite field and related equilibria. *J. Amer. Chem. Soc.* **67**, 1398-1412.

- & — (1946): The system iron–oxygen. II. Equilibrium and the thermodynamics of liquid oxide and other phases. *J. Amer. Chem. Soc.* 68, 798-816.
- ELLIOT, W.C., ULMER, G.C., GRANDSTAFF, D.E. & GOLD, D.P. (1981): A graphite–platinum association in layered intrusives? *Amer. Geophys. Union Trans.* 62, 421 (abstr.).
- EUGSTER, H.P. & WONES, D.R. (1962): Stability relations of the ferruginous biotite, annite. *J. Petrology* 3, 82-125.
- FRENCH, B.M. (1971): Stability relations of siderite (FeCO_3) in the system Fe–C–O. *Amer. J. Sci.* 271, 37-78.
- & EUGSTER, H.P. (1965): Experimental control of oxygen fugacities by graphite–gas equilibria. *J. Geophys. Res.* 70, 1529-1539.
- GEIJER, P. (1931): The iron ores of the Kiruna type. *Sveriges Geol. Undersok., Sect. C* 24, 1-39.
- GIBBON, D.L. & TUTTLE, O.F. (1967): A note on the system $\text{FeO}-\text{Fe}_2\text{O}_3-\text{SiO}_2-\text{H}_2\text{O}$. *Amer. Mineral.* 52, 886-889.
- GREIG, J.W., POSNJAK, E., MERWIN, H.E. & SOSMAN, R.B. (1935): Equilibrium relationships of Fe_3O_4 , Fe_2O_3 and oxygen. *Amer. J. Sci.* 230, 239-316.
- HAGGERTY, S.E. (1970): The Laco magnetite lava flow, Chile. *Carnegie Inst. Wash. Year Book* 68, 329-330.
- (1976): Opaque mineral oxides in terrestrial igneous rocks. In *Oxide Minerals* (D. Rumble III, ed.). *Mineral. Soc. Amer. Short Course Notes* 3, Hg101-300.
- HENRIQUEZ, F. & MARTIN, R.F. (1978): Crystal growth textures in magnetite flows and feeder dykes, El Laco, Chile. *Can. Mineral.* 16, 581-589.
- HANSEN, M. & ANDERKO, K. (1958): *Constitution of Binary Alloys*. McGraw-Hill, New York.
- HELZ, R.T. (1976): Phase relations of basalt in their melting ranges at $P_{\text{H}_2\text{O}} = 5 \text{ kb}$. II. Melt compositions. *J. Petrology* 17, 139-193.
- HOLLISTER, V.F. (1980): Origin of graphite in the Duluth complex. *Econ. Geol.* 75, 764-766.
- LINDSEY, D.H. (1976): Experimental studies of oxide minerals. In *Oxide Minerals* (D. Rumble III, ed.). *Mineral. Soc. Amer. Short Course Notes* 3, L161-184.
- LISTER, G.F. (1966): The composition and origin of selected iron–titanium deposits. *Econ. Geol.* 61, 275-310.
- LUNDBERG, B. & SMELLIE, J.A.T. (1979): Painirova and Mertainen iron ores: two deposits of the Kiruna iron ore type in northern Sweden. *Econ. Geol.* 74, 1131-1152.
- MAINWARING, P.R. & NALDRETT, A.J. (1977): Country rock assimilation and the genesis of Cu–Ni sulfides in the Water Hen intrusion Duluth complex, Minnesota. *Econ. Geol.* 72, 1269-1284.
- MUAN, A. (1955): Phase equilibria in the system $\text{FeO}-\text{Fe}_2\text{O}_3-\text{SiO}_2$. *Amer. Inst. Metals Trans.* 203, 965-976.
- (1958): Phase equilibria at high temperatures in oxide systems involving changes in oxidation states. *Amer. J. Sci.* 256, 171-207.
- (1963): Silver–palladium alloys as crucible material in studies of low-melting iron silicates. *Amer. Ceram. Soc. Bull.* 42, 344-347.
- PARK, C.F., JR. (1961): A magnetite “flow” in northern Chile. *Econ. Geol.* 56, 431-436.
- (1972): The iron ore deposits of the Pacific basin. *Econ. Geol.* 67, 339-349.
- PHILPOTTS, A.R. (1967): Origin of certain iron–titanium oxide and apatite rocks. *Econ. Geol.* 62, 303-315.
- PIWINSKII, A.J. (1974): Experimentelle Untersuchungen an granitischen Gesteinen von den südlicher Coast-Ranges, Transverse-Ranges und der Mojave-Wüste, Kalifornien. *Fortschr. Mineral.* 51, 240-255.
- SCHREINEMAKERS, F.A.H. (1915-1925): In-, mono- and divariant equilibria. *Koninkl. Akad. Wetenschappen te Amsterdam*. Collection of papers reprinted (1965) by The Pennsylvania State University, University Park, Pa.
- TAYLOR, R.W. (1963): Liquidus temperatures in the system $\text{FeO}-\text{Fe}_2\text{O}_3-\text{TiO}_2$. *J. Amer. Ceram. Soc.* 46, 276-279.
- TUTTLE, O.F. (1949): Two pressure vessels for silicate–water studies. *Geol. Soc. Amer. Bull.* 60, 1727-1729.
- WEIDNER, J.R. (1972): Equilibria in the system Fe–C–O. I. Siderite–magnetite–carbon–vapor equilibrium from 500 to 10,000 bars. *Amer. J. Sci.* 272, 735-751.
- WILLIAMS, R.J. (1971): Reaction constants in the system $\text{Fe}-\text{MgO}-\text{SiO}_2-\text{O}_2$: intensive parameters in the Skaergaard intrusion, East Greenland. *Amer. J. Sci.* 271, 132-146.
- YODER, H.S., JR. (1950): High–low quartz inversion up to 10,000 bars. *Amer. Geophys. Union Trans.* 31, 827-835.
- & TILLEY, C.E. (1962): Origin of basalt: an experimental study of natural and synthetic rock systems. *J. Petrology* 3, 342-532.

Received January 1982, revised manuscript accepted April 1982.